NCREE NEWSLETTER

March 2013 VOL. 8 NO. 1



CONTENTS

- Development of Near-Fault Factor for Design Earthquake
- Investigation and Analysis of Microtremor in Kaohsiung and Pingtung
- Micro-Earthquake Monitoring in Chianan Region, Taiwan
- Monitoring in Tatun Volcanic Group using the SSNTD Technique
- In-situ Experiment on Bridges in the Wugu-Yangmei Overpasses
- Dazhi Bridge Safety Monitoring Demonstration Project
- 5th International Conference on Advances in Experimental Structural Engineering

DIRECTOR

Kuo-Chun Chang

EDITORS

Wen-Yu Jean

Che-Min Lin

National Center for Research on Earthquake Engineering

Development of Near-Fault Factor for Design Earthquake

Yu-Wen Chang, Shyh-bin Chiou, Wen-Yu Jean, NCREE

Near-fault seismic ground motions are frequently characterized by intense peak ground accelerations and pulse-like velocity of relatively long period that clearly distinguish them from typical far-field ground motions, and cause much more damage. Understanding ground motions in near-fault regions is important for seismic risk assessment in populated areas that overlay fault zones.

After the 1999 Chi-Chi (Taiwan) earthquake, a normalized near-fault design response spectrum for sites near Type I active faults was developed based on the Taiwan seismic design code. Previously, two near-fault factors, N_A and N_V, were defined for the short period (acceleration control) and long period (velocity control) domains, because the effect is substantially greater at longer periods. Based on probabilistic seismic hazard analysis, the design requirements for structures is defined with seismic hazard levels of 10% and 2% probabilities of exceedance within 50 years (return periods of 475 years and 2,500 years). For the corresponding seismic hazard levels, the seismic hazard contribution from area sources is a reference for developing the near-fault factors of active faults. In the current Taiwan seismic building code, the reference spectral response accelerations at spectral periods of 0.3 second and 1 second for return periods of 475 years and 2,500 years are (0.8, 0.45) and (1.0, 0.55). Seven Type I active faults, which were published by the Central Geological Survey (CGS) in 2000, have been defined with near-fault factors, N_A and N_V, by the above assumption and from the results of seismic hazard analysis.

In 2010, the Bulletin of the CGS presented a revised active fault distribution according to new evidence from paleo-seismology investigations. It summarizes that there are a total of 33 active faults including both nine Type I and twenty-four Type II in Taiwan. This paper aims at developing the near-fault factors for Type I active faults in order to consider near-fault effects on the seismic demands specified in design specifications.

Because the seismic hazard analysis must account for the spatial and temporal randomness of earthquake occurrences, the influence of the differences in seismicity and active fault characteristics on the near-fault factors is self-evident. Therefore, for a particular site, especially near the fault, a deterministic approach to seismic hazard assessment is used to decide the seismic demand. This method defines a maximum credible earthquake (MCE) in terms of magnitude and distance and then calculates the ground-motion value by attenuation models. For maintaining the near-fault factors in the present seismic building code, a reduction factor will be calculated based on the prime results of seismic hazard analysis and the deterministic approach.

For near-fault zone (R = 2 km), the reduction factor η is defined as:

$$\eta(E_b, T_c) = \frac{PSHA(E_b, M_c, T_c, R)}{DSHA(M_c, R)} \qquad (1)$$

where E_b is the area source effect, and M_c and T_c are the magnitude and return period of the fault, respectively. Figure 1 shows the distribution of reduction factors of available faults in return periods of 475 and 2,500 years. The available faults are classified into three groups according to return periods of 100–400 years, 700–1000 years, and greater than 1000 years, respectively. Based on information from paleo-seismological studies, the additional faults in the 2010 bulletin can conservatively be categorized using the same criterion. It is a fact that the reduction factor is a concept of the specific ratio used in the procedure to define the near-fault factor for additional faults.

The near-fault factor for the Chishan fault is proposed and shown in Figure 2. The return period of the Chishan fault belongs to the 3rd group (> 1000 years) due to lack of information. By applying both the deterministic approach and reduction factor to the design requirements with respect to the spectral response accelerations (0.8, 0.45) and (1.0, 0.55), the near-fault factor can be calculated. The proposed reduction factor to avoid a substantial modification in the current seismic design code is appropriate at present.

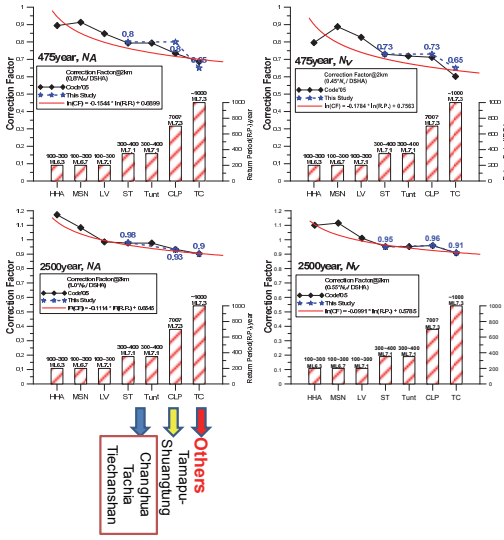


Fig. 1. The distribution of reference reduction factors for earthquakes with return periods of 475 and 2500 years

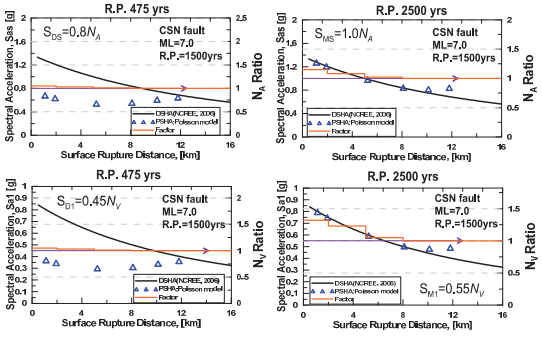


Fig.2. The near-fault factors N_A and N_V for the Chishan fault

(Yu-Wen Chang, ywchang@ncree.narl.org.tw)

Investigation and Analysis of Microtremor in Kaohsiung and Pingtung

Chun-Hsiang Kuo, Che-Min Lin, Hung-Hao Hsieh, NCREE
Kuo-Liang Wen, National Central University

Microtremors, the so-called ambient noise, are caused by various natural and artificial sources. Wind, rain, tides, traffic, and machinery are all examples of microtremor sources. The energy of the noise is relatively small compared to that of earthquakes, and the measurement time is quite short as microtremors occur constantly. Site effects are an important issue in seismology, earthquake engineering, and seismic hazard analysis. Seismic waves might be amplified at specific frequencies owing to near-surface geology, so the evaluation of site effects is a significant subject in strong-motion predictions.

In order to more effectively and precisely use collected strong motion recordings in seismology and earthquake engineering, the NCREE and the Central Weather Bureau (CWB) have operated the free-field strong motion drilling project to help construct the Engineering Geological Database for TSMIP (EGDT) since 2000 (http://egdt.ncree.org.tw/). A total of 483 free-field strong motion stations have been surveyed (Kuo *et al.*, 2011; 2012). In order to study site effects more exactly using microtremors, a study last year used logging and microtremor data at strong motion stations in the Taipei region to analyze quantitative and qualitative properties. This study introduced surveys and preliminary results in the Kaohsiung and Pingtung (KAU) regions in southwest Taiwan.

The SAMTAC-801B recorder and the VSE-331C sensor were used to conduct measurements of microtremors at the KAU strong motion stations in the KAU region. An 18-minute-long continuous recording with a sampling rate of 200 Hz is performed in each measurement. The seismograph was located close to the borehole to ensure that the geological conditions were identical. According to previous results (Kuo *et al.*, 2012), microtremors were measured at six class B stations, nine class C stations, forty-three class D stations, and two class E stations, as shown in Fig. 1.

Nakamura (1989) proposed the Horizontal-to-Vertical Spectral Ratio (HVSR) method to eliminate the effects of Rayleigh waves caused by near-surface layers and to estimate the transfer function at a certain site. The initial transfer function of a site is given by $S_T=S_{HS}/S_{HB}$ (horizontal spectrum at surface/horizontal spectrum at bedrock), and the vertical effect caused by Rayleigh waves is given by $E_S=S_{VS}/S_{VB}$ (vertical spectrum at surface/vertical spectrum at bedrock), under the assumption that the horizontal and vertical effects of Rayleigh waves are analogous. Otherwise, according to results from the observation of downhole seismographs, which indicate that horizontal and vertical spectra are almost the same, the precise transfer function (S_{TT}) can be extracted from $S_{TT}=S_T/E_S=S_{HS}/S_{VS}$ (horizontal spectrum at surface/vertical spectrum at surface).

This study measured microtremors at sixty stations with velocity profiles. The HVSRs of the stations were plotted using colors corresponding to the Vs30 measurements of the stations (Fig. 2). We can see the gradual variation of dominant frequencies from low to high with the changes of colors from yellow to green to blue. It is noted that the dominant frequency has a positive correlation with Vs30. A further study using HVSRs to estimate the site effect parameter will be undertaken in the near future.

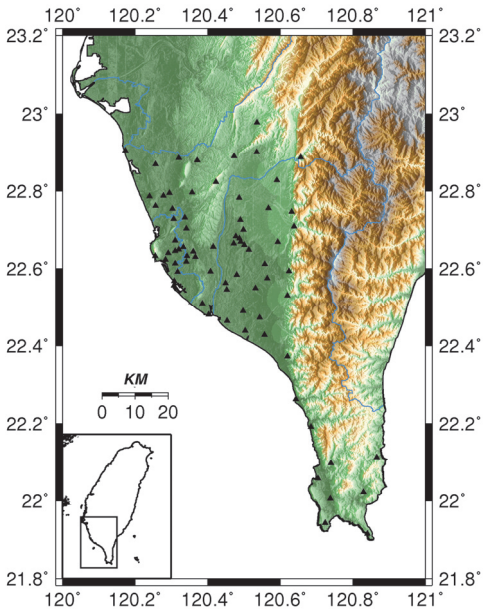


Fig. 1. The surveyed strong motion stations in the KaoPing region

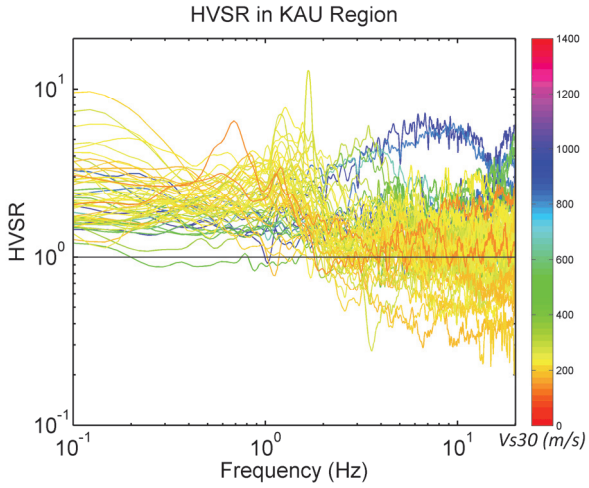


Fig. 2. HVSR curves at strong motion stations in the KaoPing region. The colors of the curves are given according to the measured Vs30

(Chun-Hsiang Kuo, chkuo@ncree.narl.org.tw)

Micro-Earthquake Monitoring in Chianan Region, Taiwan

Che-Min Lin, Hung-Hao Hsieh, Yi-Zen Chang, Chun-Hsiang Kuo, NCREE

Scattered across the Chiayi and Tainan (Chianan) regions in southwestern Taiwan are several active faults, which have induced massive earthquakes. The seismicity in general is quite high and widespread in this region. More potentially disastrous earthquakes are expected in the near future. This study aims to monitor micro-earthquake activity in the Chianan region over three years. It will monitor not only the active faults, but also blind faults and other seismogenic structures beneath the wide coastal plain. The micro-earthquakes will help us to understand the probable fault planes and rupture mechanisms of major faults.

The micro-earthquake monitoring network in the Chianan region was planned based on the distributions of historical earthquakes and major faults. Twenty-one stations were installed to develop the network in the second half of 2011. A standard operating procedure was created to avoid artificial noise. The station locations were all chosen with caution and took into account the background noise to ensure the data quality. Then, the seismometer, set in a bucket, was buried at a depth of at least 1 meter. The buckets were coupled with the ground by cement and long nails to increase the quality of the incident seismic waves. In the network, high-sensitivity broadband seismometers (CMG-6TD, Guralp System Ltd) were used to collect the weak seismic waves. A set of solar energy equipment and a GPS antenna were installed at each station to supply electricity and correct the internal clock of the seismometer. The photos in Fig. 1 show two stations installed in the field.



Fig. 1. Photos of two stations installed in the Chianan region

In addition, several real-time stations were also installed in the Chianan region. Each real-time station was installed with a broadband velocimeter and an accelerometer. The combined monitoring data provides complete ground motion information for the region. Figure 2 shows the distributions of all seismic stations installed in this study. The micro-earthquake monitoring network, which covers the Chiayi County and City, Tainan City, and adjacent foothills covered by faults, provides the complete ability to monitor the seismicity of the Chianan region.

The data quality inspection and *in situ* equipment calibration of the Chianan micro-earthquake monitoring network were done during the first two months of operation. All stations continued to record high-quality ground motion data. Every two months, the data were collected and processed to locate the observed micro-earthquakes. The monthly micro-earthquake activity was compared with the Central Weather Bureau (CWB) seismic catalog to assess the current status and variation of seismicity in the Chianan region.

Figure 2 also shows the distribution of micro-earthquakes located by the Chianan network before November, 2012. The micro-earthquakes observed in this year exhibited a widespread and frequent distribution within the monitoring scope of the network, as expected. In the northern part of the monitoring region, the Chiayi region, the earthquakes concentrated in the eastern side of the Tachienshan and Chukou Faults. Some earthquakes also took place east of Chiayi City. Meanwhile, the seismicity was quiet near the Meishan and Hsinhua Faults, which were dislocated and have induced destructive earthquakes in the past.

In Tainan City in the southern part of the region, high seismicity is heavily located along the Chukou, Muchiliao, and Liuchia Faults and extends to the southeast of the northern Chishan Fault. Earthquakes occurred on both side of these faults and were concentrated uniformly along the fault traces to form a wide seismic zone. The high seismicity may result from the broken local structure.

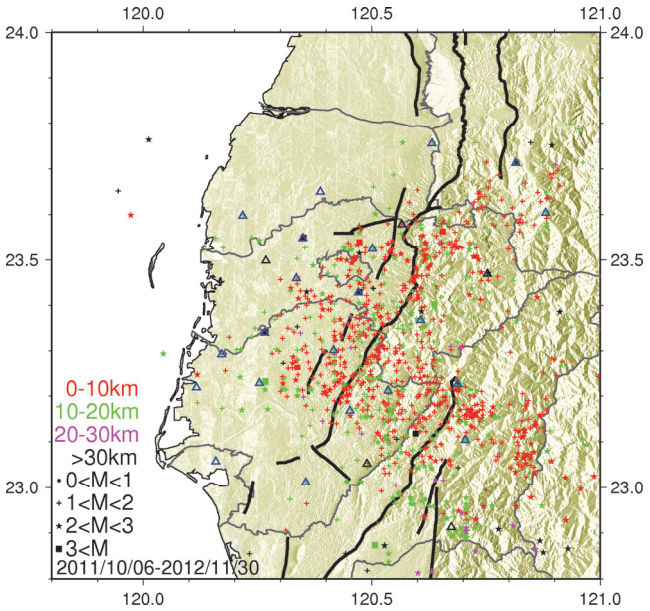


Fig. 2. Distributions of the Chianan micro-earthquake monitoring network (triangles) and the earthquakes located by it before November, 2012

(Che-Min Lin, cmlin@ncree.narl.org.tw)

Monitoring in Tatun Volcanic Group using the SSNTD Technique

Vivek Walia, Arvind Kumar, Hsiao-Hsien Chang, Shih-Jung Lin, NCREE
Tsanyao Frank Yang, National Taiwan University

The variation of volcanic gas compositions is considered to be an important index of volcanic activity. The composition of volcanic gases can help in understanding the sources and origin of magma in a particular area. Radon (^{222}Rn) is the major radioactive gas in volcanic areas. The Monitoring of radon–thoron concentrations is considered to be a useful tool to investigate the volcanic activity as well as earthquake precursory study. Three monitoring stations have already been placed in the Hsinchu, Tainan, and I-lan areas of Taiwan for earthquake forecasting studies (see previous reports). In this study, we investigate geochemical variations in the soil–gas radon–thoron concentrations using a Solid-State Nuclear Track Detector (SSNTD) technique (*i.e.*, cellulose nitrate LR-115 films) to observe the tectonic activity in the Tatun Volcanic Group (TVG) of northern Taiwan.

To carry out the present investigation, some laboratory experiments were performed where alpha track detectors were used in two modes of exposure: (i) in bare-mode and (ii) in cup-mode calibrated cellulose nitrate alpha detector films. An attempt was made to calibrate radon–thoron discriminative cups with LR-115 for simultaneous measurements of radon and thoron. Laboratory experiments have shown that progeny nuclides affect track formation in LR-115 films in the bare mode, which must be controlled in an experimental setup.

After calibration, radon–thoron discriminators along with LR-115 films were installed in the TVG (Fig. 1) at Hsiaoyoukeng (SYK), Dayoukeng (DYK), and Gungtzeping (GTP). The discriminators were installed inside the hole in the soil (about 50 cm deep) each with different temperatures for a defined period (bi-weekly to monthly) to observe possible radon–thoron flux changes to monitor volcanic and seismic activities in the area.

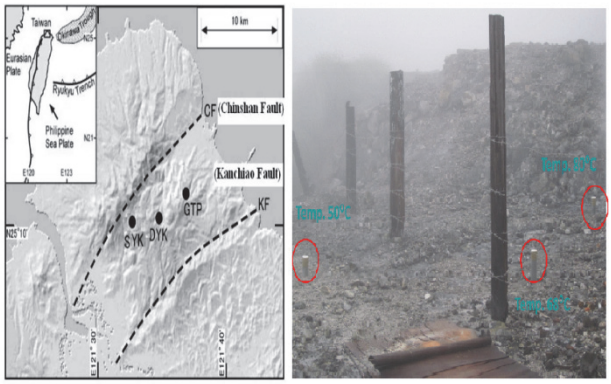


Fig. 1. Locations of monitoring stations, and locations of discriminators installed at one of the monitoring stations

Field observations have shown that the temperatures at the sites are not constant in volcanic areas; *i.e.*, the temperatures during installation and during retrieval of the films from each hole are different. The safest temperature for installing the films in volcanic areas is ≤ 65 °C. The lowest values of radon concentration were recorded at the SYK (Fig. 2) and DYK sites (Fig. 3), whereas the values of radon were comparatively high at the GTP site (Fig. 4). The low values of radon concentration at the SYK and DYK sites may be due to the existence of a magma chamber beneath them, and the area being dominated by volatile gases.

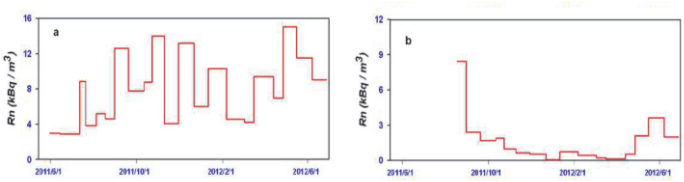


Fig. 2. Recorded average radon concentrations at SYK where: (a) temperature ranged from 24 °C to 29 °C, and (b) temperatures ranged from 48 °C to 60 °C

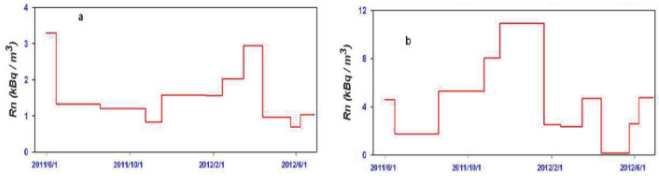


Fig. 3. Recorded average radon concentrations at DYK where: (a) temperatures ranged from 23 °C to 46 °C, and (b) temperature ranged from 60 °C to 65

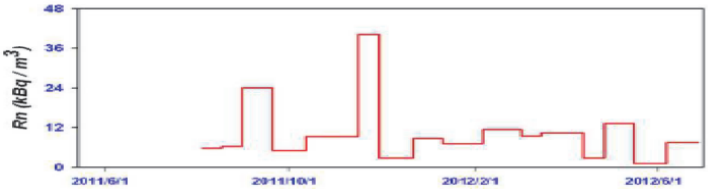


Fig. 4. Recorded average radon concentration at GTP where temperatures ranged from 35 °C to 60 °C

High values of radon at GTP may be due to the fractured zones, suggesting that the degassing sources for the TVG gases were closely related to the subduction process in north-east Taiwan. Furthermore, the observed radon behavior is different at different sites, and some sites are not suitable for radon detection. Observations have also shown potential precursory signals for some earthquakes that occurred during the observation period (January 2012 – January 2013) having an epicenter in and around the TVG (Fig. 5).

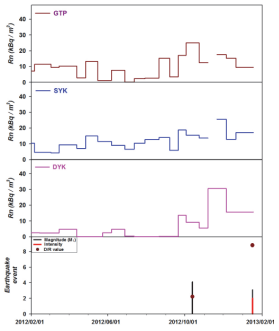


Fig.5. Variations of radon at GTP, SYK & DYK monitoring stations and their correlation with earthquakes

(walia@ncree.narl.org.tw)

In-situ Experiment on Bridges in the Wugu-Yangmei Overpasses

Yu-chi Sung, Yi-Tsung Chiu and Ta-Hsin Chang, National Taipei University of Technology
Tzu-Kang Lin, National Chiao Tung University
Hsiao-Hui Hung, Chun-Chung Chen, Chun-Lung Chen, NCREE

In the widening project area from Wugu to Yangmei (Wugu-Yangmei Overpasses) of National Highway No.1, the distance from Wugu (31 k) to Linkou (45 k) is about 14 km. There are three special bridge modules in this section of highway construction, the first special bridge modus has a long span striding across the existing roadway of Highway No.1, the second type is an F-bent double decked bridge, and the third is the steel-prestressed concrete mixed bridge structure. The forced vibration test, static loading test and dynamic loading test were conducted at bridge sites to grasp dynamic behavior of the actual structural characteristics, such as natural frequencies and vibration properties.

Experimental Configurations

Case A: A Freeway-crossing Bridge of Dual Steel Box Girders with a Main Span of 216 m

In order to reduce the environmental impact on geologically sensitive areas, the northward overpasses have to leap the existing roadway of National Highway No. 1. The length of the main span of the leaped bridge is 216 m, which includes the current largest steel box beam in Taiwan.

A-1-Force Vibration Test: Six velocity sensors were placed between piers P4A01 and P4AP2 and an accelerometer was deployed at the middle of the span. This experiment temporarily installed a shaker to force input vibrations with a frequency range from 0.3 Hz to 9 Hz, and measured the output responses of the tested bridge.

A-2-Static Truck Loading Tests: Eight cases were considered in the static loading test; the test deployed twelve 20-ton trucks on the bridge between piers P4A01 and P4A02, and also conducted leveling on the deck in this test.



Fig. 1. The testing site

A-3-Dynamic Truck Loading Tests: A series of dynamic truck loading tests, including three cases of trucks driving at speeds of 20 km/hr, 40 km/hr, and 60 km/hr, were conducted separately. In the tests, two trucks moved in parallel on either side of the bridge for each case.

In this test, a Position Sensitive Device (PSD) was applied to measure the displacement of the bridge under the loading condition.

Case B : F-bent Double-Decked Freeway Bridge

B-1-Force Vibration Test: The experiment set three sensors at the halfway, quarter-way and the end points of each upper layer and lower layer between piers P333 and P334, and deployed an accelerometer in the middle of the upper layer.

B-2-Static Truck Loading Tests: The test included seven cases of truck loading locations, and the range of the loading test was between the span of P333–P334 and the span of P334–P335.

B-3-Dynamic Truck Loading Tests: Three different cases were conducted in this test, with trucks driving at speeds of 20 km/hr, 40 km/hr, and 60 km/hr. In the test, two trucks moved in parallel on either side of the bridge for each case, and a PSD was used to measure the displacement.

Case C: Mixed Structure Bridge of Steel and Prestressed Concrete

C-1-Force Vibration Test: The experiment deployed eight velocity sensors between piers P165 and P166 and an accelerometer in the middle of the span.

C-2-Static Truck Loading Tests: The test included eight cases and was performed between piers P165 and P166, and the level of the bridge surface was also measured to obtain the deflection.

C-3-Dynamic Truck Loading Tests: The tests were performed between piers P164 and P177, and included three different cases of trucks moving at speeds of 20 km/hr, 40 km/hr, and 60 km/hr. In the test, two trucks moved in parallel on either side of the bridge for each case, and a PSD was used to measure displacements.

All tests in the project have been completed, and the analysis of measured data has begun. The results will be used to verify and calibrate the theoretical FEM model. Furthermore, this project also installed some permanent sensors for long-term monitoring, which can help to build an early-warning system for further studies.

(Chun-Chung Chen, ccchen@ncree.narl.org.tw)

Dazhi Bridge Safety Monitoring Demonstration Project

Zheng-Kuan Lee, Associate Researcher, NCREE

Introduction

Technology for the real-time monitoring of bridge safety is required by bridge management authorities and one task the National Center for Research on Earthquake Engineering (NCREE) has continually researched and developed. How to conduct real-time monitoring of long-range, multi-span bridges economically and effectively has remained the most significant challenge for related research and development. The NCREE has significantly improved the manufacturing of fiber optic sensor instruments, fiber optic welding technology, and communication capabilities in recent years, allowing the center to conduct real-time monitoring of long-range, multi-span bridges. Last September NCREE obtained approval from the Taipei City government to establish a fiber optic monitoring system on Dazhi Bridge. We hope that by using this project as an example, we can introduce a new generation of comprehensive full-bridge fiber optic monitoring technology to bridge management authorities throughout Taiwan.

Introducing Dazhi Bridge

Dazhi Bridge crosses the Keelung River, connecting to Binjiang Street in the south and Dazhi District in the north. It is an important bridge in the Zhongshan District of Taipei City. The bridge was completed and opened to traffic on June 23, 2002. Dazhi Bridge is beige with a total of 11 spans. The three spans in the north are box-shaped steel beams and the five spans in the south are pre-stressed concrete box-shaped beams. The middle three spans are fishing rod-style cable-stayed steel beams. The cable-stayed bridge section features striking red steel cables, and is considered a landmark of Taipei (Fig. 1).



Fig. 1. Dazhi Bridge landscape

Introducing the Comprehensive Full-Bridge Fiber Optic Monitoring System Developed by the NCREE

To fulfill the safety monitoring requirements for long-range, multi-span bridges, the NCREE developed a comprehensive full-bridge fiber optic monitoring system following years of research, development, and integration. The goal was to assist bridge management authorities in controlling the state of bridge safety at all times, which includes managing the flood levels, expansion joint distance changes, bridge elevation, the steel cable tension of the cable-stayed section, and other monitoring data directly related to safety (Fig. 2).

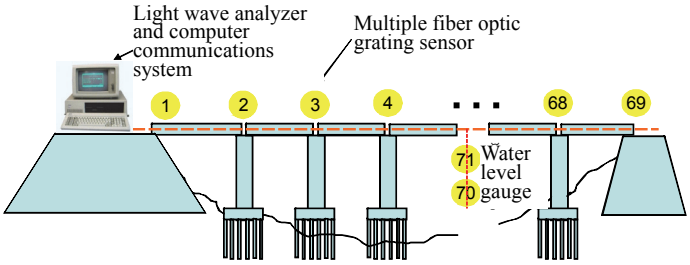


Fig. 2. Long-range, multi-span bridge safety monitoring system

The comprehensive full-bridge fiber optic monitoring system can be used to monitor bridges for (1) routine bridge testing operations; (2) earthquake and post-earthquake bridge safety; and (3) flooding and post-flood bridge safety. This monitoring system can be considered specifically designed for disaster prevention and rescue management (Fig. 3).

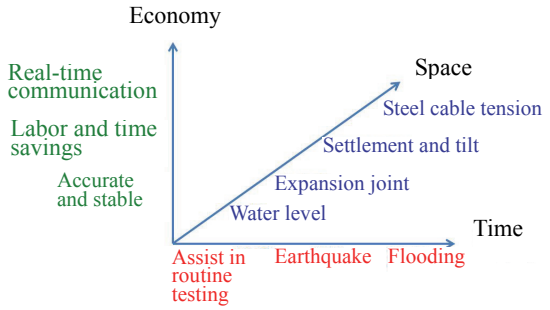


Fig. 3. Monitoring system characteristics

Introducing Fiber Optic Settlement and Tilt Sensor Gauge

Fiber optic settlement and tilt sensor gauge can monitor bridge elevation, which is the monitoring system's most prominent characteristic. This system applies the communicating vessels principle and the buoyancy principle to monitor changes in bridge elevation (Fig. 4). According to the design dimensions, the instrument accuracy is up to 1 mm, and the high resolution is extremely beneficial for monitoring the bridge pier settlement or tilt.

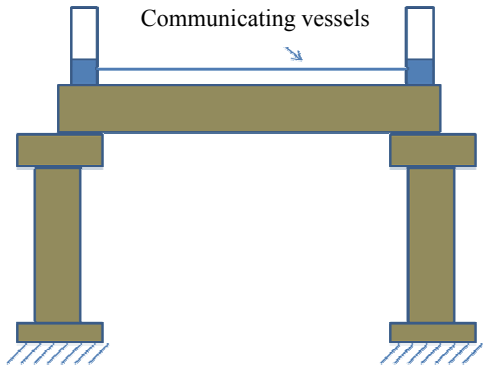


Fig. 4. Fiber optics settlement and tilt sensor gauge

Layout of the Comprehensive Full-Bridge Fiber Optic Monitoring System for Dazhi Bridge

The NCREE installed steel cable vibration meters, bridge altimeters, angle gauges, expansion joint displacement meters, and flood level gauges throughout Dazhi Bridge.

Monitoring Data Analysis

After transmission to the NCREE, real-time monitoring data are immediately analyzed. The monitoring data are illustrated in Fig. 5. The top image is the vibration of the longest steel cable, the middle image shows the rotation of the girder, and the bottom image shows the elevation of the girder. Dynamic messages are rendered in real-time.

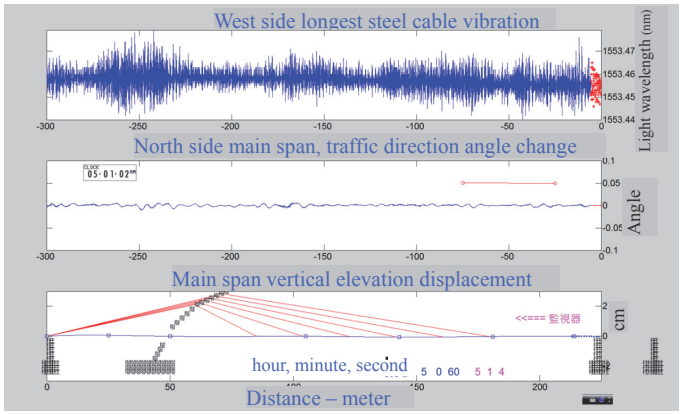


Fig. 5. Illustration of monitoring data: the top image shows the steel cable vibration, the middle image shows the girder's rotation, and the bottom image shows the girder's elevation profile.

Conclusion

After many years of research, development and system integration, the NCREE can finally self-produce sensors and integrate communication systems, facilitating the achievement of long-range, multi-span bridge safety monitoring.

(Zheng-Kuan Lee, zklee@ncree.narl.org.tw)

5th International Conference on Advances in Experimental Structural Engineering

NCREE is currently organizing the 5th International Conference on Advances in Experimental Structural Engineering (5AESE). The conference is to be held in NCREE, Taipei, Taiwan, on 8-9 November, 2013.

Themes:

1. Novel testing, measuring, and monitoring techniques in structural/geotechnical engineering
2. Real time structural testing techniques
3. Hybrid simulations
4. Modeling and numerical simulation in predicting and interpreting experimental results
5. Standardization of testing procedures
6. Application of experimental results to structural design and analysis
7. Data management and information systems for structural experimentation
8. Design, construction, and utilization of novel testing facilities
9. Software and hardware development for structural experiments

Important dates:

Deadline for abstract submission: 31 March, 2013

Notification of abstract acceptance: 15 April, 2013

Deadline for paper submission: 15 August, 2013

Contact: 5aese@ncree.narl.org.tw

Website: aese5.ncree.narl.org.tw

Published by

National Center for Research on Earthquake Engineering

200, Sec. 3, XinHai Rd., Taipei 106, Taiwan, R.O.C.

Phone: 886-2-6630-0888

Fax: 886-2-6630-0858

Website: http://newsletter.ncree.org

The National Center for Research on Earthquake Engineering (NCREE) is a laboratory of National Applied Research Laboratories (NARL)

Website: http://www.narl.org.tw